Surface plasmons in two-sided corrugated thin films

S. Dutta Gupta, G. V. Varada, and G. S. Agarwal
School of Physics, University of Hyderabad, Hyderabad 500 134, Andhra Pradesh, India
(Received 23 April 1987)

Coupled surface plasmons in a thin free-standing metal film with both the interfaces periodically corrugated are studied. Infinite Rayleigh expansions in terms of the spatial harmonics with proper boundary conditions are used to obtain the infinite hierarchy of coupled amplitude equations. The truncated system of equations is numerically solved to explain the experimental results of Inagaki *et al.* [Phys. Rev. B **32**, 6238 (1985)]. The theoretical investigation goes beyond the range of the parameters used in the experiment and we reveal the nonperturbative character of the peak intensities as a function of the corrugation amplitude.

I. INTRODUCTION

The coupling of surface plasmons in a thin metal film has been the subject of considerable theoretical and experimental interest.[1,2] For thin metal films the coupling results in the bifurcation of the dispersion curve in two distinct branches, one corresponding to the long-range surface plasmons and the other to the short-range surface plasmons. Compared to the short-range surface plasmons, the long-range surface plasmons are characterized by a larger propagation length. The excitation of the surface plasmons and especially long-range surface plasmons leads to very large local fields[3] which makes them suitable candidates for low-threshold nonlinear optical phenomena.[4,5]

In a recent series of experiments[6,7] Inagaki *et al.* have studied the dispersion characteristics of the coupled modes in a free-standing corrugated Ag film using photoacoustic techniques. For the chosen experimental parameters the results are strikingly close to the flat-surface calculations. The major difference between the experimental observations and the flat-surface calculations is in the decay length of the surface modes. Besides, the experimental studies reveal a/d (where a is the corrugation amplitude and d is half the width of the film) as a crucial parameter for the total intensity.

In the experiment it was difficult to make films with large a. Therefore it was not possible to observe the effects of radiation damping on the surface modes. In short, most of the experimental results on the dispersion relations are rather close to what one would expect for a corrugationless thin film. It is well known that for the case of a single interface, small surface corrugation introduces finite corrections to the flat-surface results. For large corrugation amplitudes, the calculation of the changes in the dispersion of the surface modes is beyond the scope of a perturbative[8-10] theory.

In this paper we present a general theory for a two-sided corrugated metal film for p-polarized incident waves. We express the fields in the three media (above, in, and below the metal film) as a superposition of all the spatial harmonics. Assuming the Rayleigh hypothesis to be valid, we demand the continuity of the surface components of the electric and magnetic fields, which yields the infinite set of coupled amplitude equations. We truncate this system and solve it numerically using the experimental parameters of Inagaki *et al.*[7] From the calculated data of the zero-order reflectivity we obtain the dispersion curves for both the long-range and short-range modes. We observe that the parameter a/d is also an important parameter determining the applicability of the Rayleigh hypothesis. Moreover, we study the system for corrugation amplitudes larger than those used in the experiment to reveal the effects due to radiation damping, i.e., due to the conversion of nonradiative surface plasmons into radiative modes.

The organization of the paper is as follows: In Sec. II we obtain the coupled amplitude equations. In Sec. III we present the results of our numerical study of the truncated system. In the same section we compare our theoretical results with the experimental observations and discuss them.

II. DERIVATION OF THE COUPLED AMPLITUDE EQUATIONS

We consider the system shown in Fig. 1. Let a plane monochromatic wave with frequency ω be incident at an angle θ on the periodically corrugated thin metal film with upper and lower surface profiles given by

$$y_{\pm}=\pm d+a\sin(Kx)\ , \tag{2.1}$$

where $K=2\pi/\Lambda$ (Λ is the grating period) is the grating vector. For p-polarized incident waves the magnetic field in various domains can be written as

$$H_{1z}=e^{i(\gamma_0 x-\beta_0 y)}+\sum_{n=-\infty}^{\infty}B_{1n}e^{i(\gamma_n x-\beta_n y)},\quad y>y_+ \tag{2.2}$$

$$H_{2z}=\sum_{n=-\infty}^{\infty}e^{i\gamma_n x}(A_{2n}e^{-i\tilde{\beta}_n y}+B_{2n}e^{i\tilde{\beta}_n y}),\quad y_-<y<y_+ \tag{2.3}$$

$$H_{3z}=\sum_{n=-\infty}^{\infty}A_{3n}e^{i(\gamma_n x-\beta_n y)},\quad y<y_-\ . \tag{2.4}$$

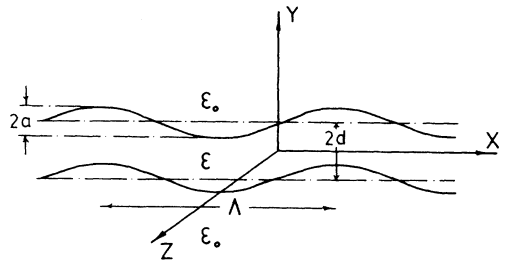

FIG. 1. Schematic diagram of the two-sided corrugated thin film with period Λ, corrugation amplitude a, and thickness $2d$.

In (2.2)–(2.4) we have assumed the incident amplitude to be unity, so that the other constant amplitudes B_{1n}, B_{2n}, and A_{2n}, A_{3n} can directly give the amplitude reflection and transmission coefficients of the nth spatial harmonic, respectively. The other parameters in (2.2)–(2.4) are given by

$$\begin{aligned}\gamma_0&=k_0\epsilon_0^{1/2}\sin\theta\ ,\\ \gamma_n&=\gamma_0+nK\ ,\\ \beta_n^2&=k_0^2\epsilon_0-\gamma_n^2\ ,\\ \tilde{\beta}_n^2&=k_0^2\epsilon-\gamma_n^2\ .\end{aligned}\tag{2.5}$$

Here γ_n is the x component and β_n, $\tilde{\beta}_n$ are the y components of the wave vector for the nth spatial harmonic. ϵ_0 ($\epsilon_0=1$) and ϵ are the dielectric constants of vacuum and metal, respectively. The corresponding electric field components in each medium can be calculated by substituting (2.2)–(2.4) in Maxwell's curl **H** equation. We now assume that the Rayleigh hypothesis is valid, i.e., the fields in the vicinity of the corrugated surface can be expressed by the Rayleigh expansions (2.2)–(2.4). The boundary conditions can be written as

$$\begin{aligned}&H_{1z}\,|_{y=y_+}=H_{2z}\,|_{y=y_+},\quad H_{2z}\,|_{y=y_-}=H_{3z}\,|_{y=y_-}\ ,\\ &(E_{1x}t_x+E_{1y}t_y)\,|_{y=y_+}=(E_{2x}t_x+E_{2y}t_y)\,|_{y=y_+}\ ,\\ &(E_{2x}t_x+E_{2y}t_y)\,|_{y=y_-}=(E_{3x}t_x+E_{3y}t_y)\,|_{y=y_-}\ .\end{aligned}\tag{2.6}$$

Here t_x and t_y are the x and y components of the unit vector **t** tangent to the surface with the form

$$\mathbf{t}=\{1+[aK\cos(Kx)]^2\}^{-1/2}(1,\ aK\cos(Kx),\ 0)\ .\tag{2.7}$$

Substituting (2.2)–(2.4) and the calculated values of E_x and E_y in (2.6) and using (2.7) we obtain the following infinite set of coupled amplitude equations with respect to the amplitudes of the spatial harmonics:

$$\sum_{n=-\infty}^{\infty}[B_{1n}e^{i\beta_n d}J_{m-n}(\beta_n a)-A_{2n}e^{-i\tilde{\beta}_n d}J_{n-m}(\tilde{\beta}_n a)-B_{2n}e^{i\tilde{\beta}_n d}J_{m-n}(\tilde{\beta}_n a)]=(-1)^{m+1}e^{-i\beta_0 d}J_m(\beta_0 a)\ ,\tag{2.8}$$

$$\begin{aligned}\sum_{n=-\infty}^{\infty}\Bigg[&B_{1n}\frac{\gamma_n\gamma_m-k_0^2\epsilon_0}{\beta_n}e^{i\beta_n d}J_{m-n}(\beta_n a)+A_{2n}\frac{\epsilon_0}{\epsilon}\frac{\gamma_n\gamma_m-k_0^2\epsilon}{\tilde{\beta}_n}e^{-i\tilde{\beta}_n d}J_{n-m}(\tilde{\beta}_n a)\\ &-B_{2n}\frac{\epsilon_0}{\epsilon}\frac{\gamma_n\gamma_m-k_0^2\epsilon}{\tilde{\beta}_n}e^{i\tilde{\beta}_n d}J_{m-n}(\tilde{\beta}_n a)\Bigg]=(-1)^{m+1}\frac{k_0^2\epsilon_0-\gamma_0\gamma_m}{\beta_0}e^{-i\beta_0 d}J_m(\beta_0 a)\ ,\end{aligned}\tag{2.9}$$

$$\sum_{n=-\infty}^{\infty}[A_{2n}e^{i\tilde{\beta}_n d}J_{n-m}(\tilde{\beta}_n a)+B_{2n}e^{-i\tilde{\beta}_n d}J_{m-n}(\tilde{\beta}_n a)-A_{3n}e^{i\beta_n d}J_{n-m}(\beta_n a)]=0\ ,\tag{2.10}$$

$$\begin{aligned}\sum_{n=-\infty}^{\infty}\Bigg[&A_{2n}\frac{\epsilon_0}{\epsilon}\frac{\gamma_n\gamma_m-k_0^2\epsilon}{\tilde{\beta}_n}e^{i\tilde{\beta}_n d}J_{m-n}(\tilde{\beta}_n a)\\ &-B_{2n}\frac{\epsilon_0}{\epsilon}\frac{\gamma_n\gamma_m-k_0^2\epsilon}{\tilde{\beta}_n}e^{-i\tilde{\beta}_n d}J_{n-m}(\tilde{\beta}_n a)-A_{3n}\frac{\gamma_n\gamma_m-k_0^2\epsilon_0}{\beta_n}e^{i\beta_n d}J_{m-n}(\beta_n a)\Bigg]=0\ ,\end{aligned}\tag{2.11}$$

where m takes all integer values between $-\infty$ and $+\infty$. In deriving Eqs. (2.8)–(2.11) we have used the following expansion for terms like $\exp[i\beta_n a\sin(Kx)]$:

$$e^{i\beta_n a\sin(Kx)}=\sum_{s=-\infty}^{\infty}e^{isKx}J_s(\beta_n a)\ .\tag{2.12}$$

Note that the use of the expansion (2.12) is equivalent to retaining all orders of the surface corrugation amplitude a. Thus the infinite system of Eqs. (2.8)–(2.11) represent the exact character of coupling between the different spatial harmonics. Hence the solution of (2.8)–(2.11) will be quite different from any finite-order perturbative results. It should be mentioned here that the validity of the set of Eqs. (2.8)–(2.11) will be determined by the validity of the Rayleigh hypothesis which was the only assumption used in obtaining them.

In Sec. III we truncate the infinite system of Eqs. (2.8)–(2.11) retaining a finite number of harmonics. Note that the truncated system includes the contributions from all orders by a virtue of the expansions (2.12) and hence is quite distinct from any perturbation method which retains only up to a finite order of a. We present our numerical results in Sec. III.

III. NUMERICAL RESULTS AND DISCUSSIONS

We truncate the system of Eqs. (2.8)–(2.11) by retaining the following harmonics:

$$-l_i, -l_i+1, \ldots, 0, \ldots, -l_i+l_f \ , \tag{3.1}$$

where l_i and l_f are positive integers. The truncated system results in a matrix equation of the form $DX=F$ with the dimension of the coefficient matrix equal to $4(l_i+l_f+1)\times 4(l_i+l_f+1)$. We solve this system numerically with the experimental parameters of Inagaki *et al.*[7] We retain five harmonics ($l_i=1$, $l_f=3$) and check the convergence by adding one more harmonic both on the negative and the positive sides. For the experimental parameters convergence was fairly good and we did not need a larger number of harmonics. Instead of examining the total intensity due to all the spatial harmonics we study separately the zero- and first-order reflected intensities (R_0 and R_{+1}, respectively) for $+1$ surface-plasmon (SP) resonance and zero-, first-, and second-order reflected intensities (R_0, R_{+1}, R_{+2}, respectively) for $+2$ surface-plasmon resonance. Note that $(+n)$-order surface-plasmon resonance is defined by the equation

$$k_0 \sin\theta + nK = k_{\mathrm{SP}} \ , \tag{3.2}$$

where k_{SP} is the SP wave vector for the corrugated surface. We present the results of the angular scanning for $+1$ SP resonance in Fig. 2. Figure 2(a) shows the dependence of R_0 as a function of θ whereas Fig. 2(b) shows the field enhancement R_{+1} as a function of θ for three different sets of the values of d and a. It is evident from these figures that for smaller film thickness, due to the coupling of the two interface plasmons, the resonance gets split into two, one corresponding to the long-range surface plasmon and the other to the short-range surface plasmon. It can be seen from Fig. 2(a) that some "dispersion"-like dependence appears near the long-range resonance dip (near $\theta=43°$). This is because of the existence[11] of a complex pole and a complex zero in R_0. The separation of the poles and zeroes and their values depend crucially on the system parameters. For the given set of parameters, they are not widely separated

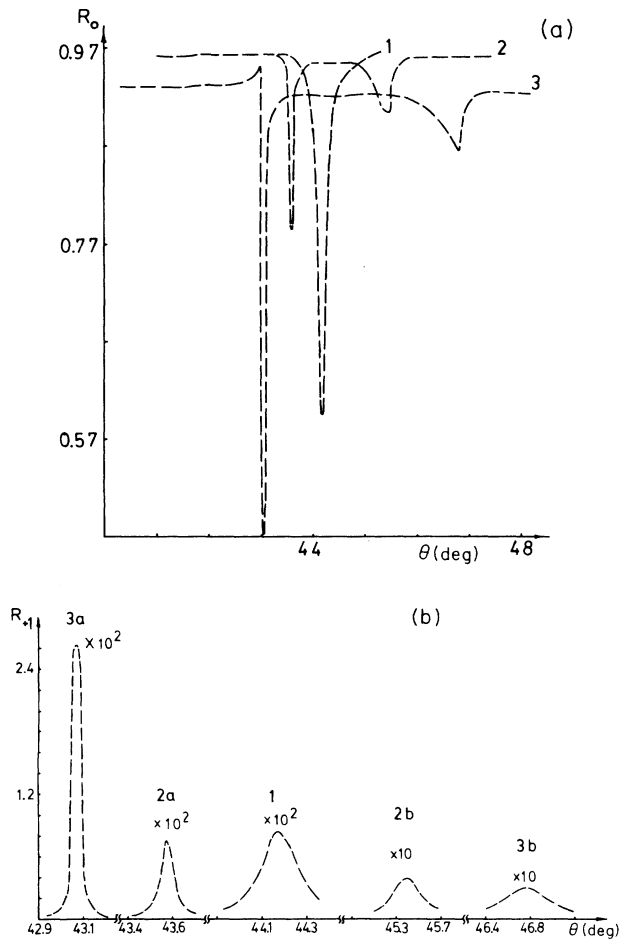

FIG. 2. (a) R_0 as a function of the angle of incidence θ for $+1$ surface-plasmon resonance for different values of a and d: (1) $d=60.5$ nm, $a=12$ nm; (2) $d=30$ nm, $a=8$ nm; (3) $d=22$ nm, $a=8$ nm. (b) R_{+1} as a function of the angle of incidence θ for $+1$ surface-plasmon resonance. Different curves are for the same sets of parameters a and d as in (a). a and b refer to the long- and short-range components, respectively.

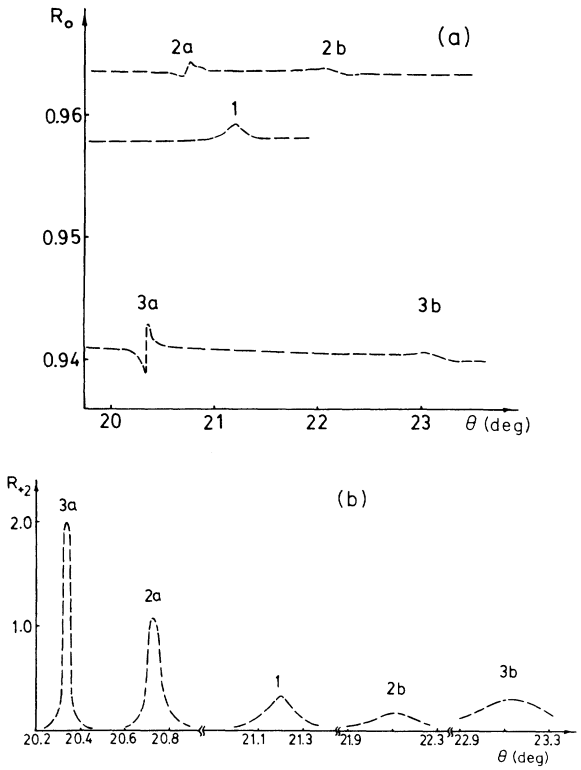

FIG. 3. (a) R_0 as a function of the angle of incidence θ for $+2$ surface-plasmon resonance. Different curves are for the same sets of parameters a and d as in Fig. 2(a). a and b refer to the long-range and short-range modes, respectively. (b) R_{+2} as a function of the angle of incidence θ for $+2$ surface-plasmon resonance. Different curves are for the same sets of parameters a and d as in Fig. 2(a). a and b refer to the long-range and short-range components, respectively.

and their contributions are significant, which explains the observed behavior. Our theoretical calculations agree well with the experimental results. However, an insignificant deviation was observed in the angular resonance positions. We ascribe this to the inaccuracy of the value of the dielectric constant ϵ (we take $\epsilon=-16.3+0.53i$ as in the work of Inagaki *et al.*) and to the deviations from the strictly periodic variation of the surface profile. Dependence of R_{+1} on θ [Fig. 2(b)] shows resonances at the same angular locations and the maximum enhancement is achieved for the thinner film ($d=22$ nm, $a=8$ nm). The $+2$ SP resonance curves (Fig. 3, where we show only R_0 and R_{+2}, respectively) shows qualitatively the same behavior as $+1$ resonance curves with the difference that the coupling efficiency is much less.

Next, we concentrate on the $+1$ SP resonance to obtain the dispersion curves for the long-range and short-range modes. For theoretical calculations we assume the a/d ratio to be constant and we have taken these values from the slope of the straight line in Fig. 1 of the work of Inagaki *et al.*[7] The values of the wave vectors k_- and k_+ for the long-range and short-range modes, respectively, were calculated by the positions of the minima of R_0 as a function of θ. It may be noted here that a better way to calculate the dispersion curve would be to use the peak positions of the local fields (R_{+1}). This is due to the fact that R_{+1}, being the evanescent mode with close to zero transverse component of the wave vector, reflects the surface excitation more accurately. However, for the parameters used in the experiment the position of minima for R_0 and maxima for R_{+1} were identical. In Fig. 4 we present the results where we have plotted $(k_+-k_-)/(\omega/c)$ as a function of the film thickness. In the same figure we have reproduced the experimental and the flat-surface results for comparison. It can be clearly seen from Fig. 4 that our theoretical calculations are very close to the flat-surface results. Minor deviations are there for larger d, when accordingly, the corrugation amplitude a is comparatively large (recall that $a/d=$const). For larger corrugation amplitudes, one would expect different results for flat and corrugated surfaces. Experimental observations are indeed very close to the flat-surface results and thus do not see the effects of the corrugation. We have not calculated the imaginary part of the wave vectors because of the difficulty in determining the resonance widths. Besides, the question which of the resonances has to be used to determine the imaginary part of the wave vectors is still open. Nevertheless, we make a guess of the decay length for the k_- mode by the resonance width of the R_{+1} curve [see Fig. 2(b)] for $d=22$ nm. It turns out to be approximately 159.7 μm. The experimental result is approximately 50.3 μm, whereas, the flat-surface calculations predict an approximate value 167.9 μm. It is clear from the above discussion that surface corrugation, though it leaves almost unaffected the real part of the propagation vector, to some extent affects the imaginary part, thereby introducing an extra loss for the surface modes. The deviations of the theoretical and experimental results are mostly due to the factors mentioned in the

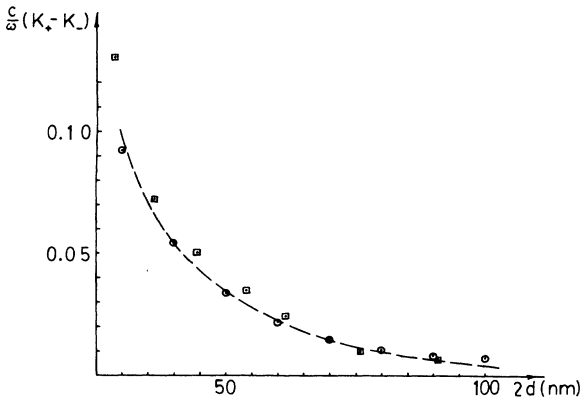

FIG. 4. $(c/\omega)(k_+-k_-)$ as a function of the film thickness $2d$. The dashed curve gives the flat-surface results. Circular dots are the theoretically calculated values and the square dots are the experimental observations.

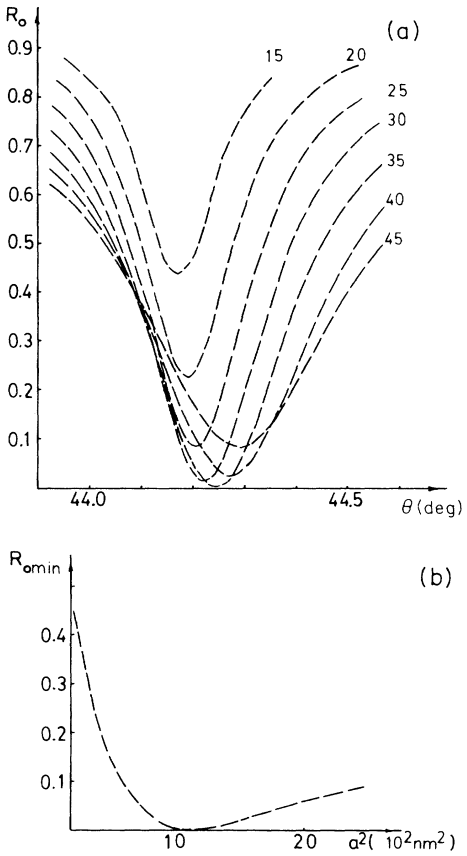

FIG. 5. (a) R_0 as a function of θ for $+1$ surface-plasmon resonance for various corrugation amplitudes. The film thickness is 102 nm. Different curves are labeled by the corresponding values of the corrugation amplitude. (b) Minimal intensity $R_{0\min}$ for $+1$ surface-plasmon resonance as a function of the square of the corrugation amplitude a^2 for a film with thickness 102 nm.

work of Inagaki *et al.*[7]

In what follows we study the effect of radiation damping, i.e., of the conversion of nonradiative surface plasmons into radiative modes, on the surface modes. For this we investigate a corrugated film with thickness $2d = 102$ nm for various corrugation amplitudes. The results are shown in Fig. 5. In Fig. 5(a) we show the dependence of R_0 as a function of θ, whereas in Fig. 5(b) we plot $R_{0\min}$ [minimal zero-order reflectivity obtained from Fig. 5(a)] as a function of the square of the corrugation amplitude a^2. It is clear from Fig. 5(b) that for a^2 values larger than 600 nm^2, significant deviations from perturbation theory, i.e., from $R_{0\min} \propto a^2$ take place. For large a the curve bends and thus shows a minimum for $a^2 \sim 1200$ nm^2. We could not study such optimal behavior for thinner films for the following reason. For the chosen wavelength and grating periodicity, the optimal coupling occurs near the region of $a = 35$ nm. This means that the a/d ratio will be very close to or greater than unity for thin films where the coupling of surface plasmons can take place. We observed that for $a/d \gtrsim 1$, no fixed pattern in the reflected intensities could be obtained. This was tested retaining a large number of harmonics (as many as 13). It appears that for $a/d \gtrsim 1$ the Rayleigh hypothesis is not valid, since along the plane $y = 0$ one encounters media with both the dielectric constants ϵ_0 and ϵ.

In conclusion we have presented a nonperturbative theoretical model for coupled surface plasmons in a periodically corrugated thin film. For actual calculations we have used the system parameters of the experiment of Inagaki *et al.* The basic conclusions of the experiment are supported by our theoretical calculations. Moreover, we investigated the optimal behavior of the extremal zero-order intensities as a function of the corrugation amplitude to reveal the importance of the parameter a/d, which determines the validity of the Rayleigh hypothesis in theoretical calculations.

ACKNOWLEDGMENTS

We are grateful to Dr. T. Inagaki for sending us the experimental data. We would also like to thank the University Grants Commission, Government of India, for supporting this work.

[1]See, for example, R. H. Ritchie and H. B. Eldridge, Phys. Rev. **126**, 1935 (1962); K. L. Kliewer and R. Fuchs, *ibid.* **144**, 495 (1966); E. N. Economou, *ibid.* **182**, 539 (1969); A. Otto, Z. Phys. **219**, 227 (1969); D. Sarid, Phys. Rev. Lett. **47**, 1927 (1981).

[2]For an excellent review on the coupling of surface plasmons, see, for example, H. Raether, *Physics of Thin Films* (Academic, New York, 1977), Vol. 9, pp. 145–261.

[3]D. Sarid, R. T. Deck, A. E. Craig, R. K. Hickernell, R. S. Jameson, and J. J. Fasano, Appl. Opt. **21**, 3993 (1982); D. Sarid, R. T. Deck, and J. J. Fasano, J. Opt. Soc. Am. **72**, 1345 (1982).

[4]For local field enhancements and their applications, see, for example, J. C. Quail, J. G. Rako, H. J. Simon, and R. T. Deck, Phys. Rev. Lett. **50**, 1987 (1983); G. S. Agarwal and S. Dutta Gupta, Phys. Rev. B **34**, 5239 (1986); R. K. Hickernell and D. Sarid, J. Opt. Soc. Am. B **3**, 1059 (1986).

[5]Local field enhancements are crucial for surface enhanced nonlinear phenomena, see, for example, D. L. Mills and W. Weber, Phys. Rev. B **26**, 1075 (1982); J. L. Coutaz, M. Neviere, E. Pic, and R. Reinisch, *ibid.* **32**, 2227 (1985); M. Neviere, R. Reinisch, and D. Maystre, *ibid.* **32**, 3634 (1985); G. S. Agarwal and S. S. Jha, *ibid.* **26**, 482 (1982); see, for example, articles by P. F. Liao, Y. R. Shen, A. Wokaun, in *Surface Studies with Lasers,* edited by F. R. Aussenegg, A. Leitner, and M. E. Lippitsch (Springer, Berlin, 1983); articles by H. Metiu, J. I. Gersten, A. Nitzan, S. S. Jha, and P. F. Liao, in *Surface Enhanced Raman Scattering,* edited by R. K. Chang and T. E. Furtak (Plenum, New York, 1982).

[6]T. Inagaki, M. Motosuga, E. T. Arakawa, and J. P. Goudonnet, Phys. Rev. B **32**, 2548 (1985).

[7]T. Inagaki, M. Motosuga, E. T. Arakawa, and J. P. Goudonnet, Phys. Rev. B **32**, 6238 (1985).

[8]For various perturbative methods in the theory of single interface gratings, see, for example, G. S. Agarwal, Phys. Rev. B **15**, 2371 (1977); F. Toigo, A. Marvin, V. Celli, and N. R. Hill, *ibid.* **18**, 5618 (1977); A. A. Maradudin and D. L. Mills, *ibid.* **11**, 1392 (1975); A. A. Maradudin and W. Zierau, *ibid.* **14**, 484 (1976); A. A. Maradudin, in *Surface Polaritons,* edited by V. M. Agranovich and D. L. Mills (North-Holland, Amsterdam, 1982), p. 405.

[9]For the perturbative treatment of the coupled modes in a layered structure, see, for example, G. S. Agarwal, Phys. Rev. B **31**, 3534 (1985); Y. Yasumoto, J. Appl. Phys. **57**, 755 (1985); O. R. Asfar and A. H. Nayfeh, Siam Rev. **25**, 455 (1983); A. H. Neyfeh and O. R. Asfar, J. Appl. Phys. **45**, 4797 (1974).

[10]For nonperturbative approaches, see, for example, A. A. Maradudin, J. Opt. Soc. Am. **73**, 759 (1983); D. Agassi and T. F. George, Phys. Rev. B **33**, 2393 (1986).

[11]M. Neviere, in *Electromagnetic Theory of Gratings,* edited by R. Petit (Springer, Berlin, 1980), p. 123.